2-Mercaptopyrimidine-functionalized mesostructured silicas to develop electrochemical sensors for a rapid control of scopolamine in tea and herbal tea infusions

Judith Gañán . Sonia Morante-Zarcero . Damián Pérez-Quintanilla . Isabel Sierra*

Departamento Tecnología Química y Ambiental, ESCET, Universidad Rey Juan Carlos C/ Tulipán s/n, 28933, Móstoles, Madrid, Spain.

* Corresponding author

E-mail addresses: isabel.sierra@urjc.es (Isabel Sierra)

ABSTRACT

Mesostructured silicas were synthesized and chemically functionalized with a 2-mercaptopyrimidine (MPY)-derivative. Bare and functionalized silicas (MSU-2, HMS, SBA-15, MSU-2-MPY, HMS-MPY and SBA-15-MPY) were characterized by powder X-ray diffraction, nitrogen adsorption-desorption isotherms, transmission electron and scanning electron microscopy, ^{29}Si and ^{13}C cross-polarization magic-angle spinning NMR spectroscopy and elemental analysis, and used to prepare modified carbon paste electrodes (CPEs). The electrodes properties were studied using potassium ferrocyanide and scopolamine as probes employing cyclic voltammetry (CV) and differential pulse voltammetry (DPV). Results proved that MPY groups on the silica surface were necessary to improve the sensitivity in the voltammetric determination of scopolamine. CPE modified with HMS-MPY exhibited higher peak current toward the oxidation of scopolamine, with a well-defined oxidation peak at + 1.1 V (vs. Ag/AgCl) in DPV. This fact can be attributed to the high electroactive area of this material, with 3 D wormhole-like channel structure that favored the scopolamine diffusion. Under optimum conditions, HMS-MPY-CPE exhibited a wider linearity range, from 0.9 to 200 μM, with a detection limit of 0.3 μM and good reproducibility by DPV. The developed sensor was successfully applied for a rapid determination of scopolamine in spiked tea and herbal tea infusion samples with good recoveries (between 83 ± 5 and 101 ± 1%).

Keywords Chemical modified carbon paste electrodes . Mesostructured silicas . 2-Mercaptopyrimidine . Electrochemical sensor . Scopolamine . Herbal teas

1. Introduction

Scopolamine (hyoscine) is one of the most abundant tropane alkaloids (TAs) produced as secondary metabolite by plants of several families, being the most common sources *Atropa belladonna* and *Datura stramonium* [1]. In recent years, there has been a growing interest in these natural toxins due to their presence as contaminants in food and feed, as they are a potential hazard for human and animal health [2]. The toxicological effects of TAs include delirium, agitation and convulsions, tachycardia, nausea and vomiting, swallowing and speaking difficulty, hypertension, loss of consciousness and may even produce coma [3]. For these reasons, in 2015 the European Commission issued a recommendation for the Member States to perform monitoring for the presence of TAs in food and feed, particularly in cereals and derivate products, oilseeds, legumes, foods supplements, gluten free products, teas and herbal infusions [4]. In the last three years, the Rapid Alert System for Food and Feed (RASFF) created by the European Commission has reported five important alerts related with the presence of high levels of TAs in herbal infusions.

Various methods have been developed for the determination of scopolamine in foods, including capillary electrophoresis [5], gas chromatography mass spectrometry [6] and liquid chromatography mass spectrometry [7-9]. These instrumental techniques can achieve high sensitivity, selectivity and good precision, but they are expensive and demands laborious and time-consuming procedures, which makes them unattractive when fast control methods are required. In this sense, electrochemical techniques can be an excellent alternative since they can achieve cost-effective and rapid analysis, with good sensitivity and selectivity, high reproducibility and accuracy, and simplified miniaturization suitable for *in-situ* measurements [10]. Regarding to published

electrochemical methods for scopolamine determination, in general, only pharmaceutical preparations and biological fluids have been analysed [11, 12]. Recently, because of the illicit use of this compound (also known as burundanga) with recreational and predatory purposes, an electrochemical method for on-site screening of scopolamine in beverages has been successfully applied using a boron-doped diamond as the working electrode [13].

During the last decade, considerable interest has focused on mesostructured silica-based sensors, which demonstrated a great potential in the electrochemical determination of trace contaminants [14]. Mesostructured silicas (MS) have excellent properties such as high thermal and mechanical stability, high surface area and large pore volume. These materials have attracted considerable interest of scientists since their discovery in electrochemical applications, due to their highly porous and regularly ordered structure, which provides good accessibility and fast mass transport to the active centers [15]. Moreover, the surface properties of these types of materials can be easily modified, and a wide variety of organic groups (e.g. amino, mercapto, sulfonic or thiol) have been immobilized on the surface of MS in a controllable manner. These immobilized groups could significantly improve the adsorption on MS due to the selective-bonding between the functional groups and the analytes. Over the last decade, these materials (unmodified as well as functionalized) have been successfully applied as carbon paste electrode (CPE) modifiers. For example, Morante-Zarcero et al. used a CPE modified with non-functionalized MS to determinate bisphenol A in water samples [16]. Different MSs (HMS and MCM-41) functionalized with amine groups were successfully used for determination of β-blockers in drinking waters [17] and Cu (II) in tea samples [18]. In other work of our research group, four different types of MSs functionalized with a 5-mercapto-1-methyltetrazole-derivative were evaluated as CPE modifiers for

voltammetric analysis of Pb (II). Results demonstrated that the analytical performance of the MS-modified CPEs (MS-CPEs) was greatly influenced by textural characteristics of the silicas, as well as that the thiol groups anchored to the MS surface improve electrochemical signal [19]. Several works have been demonstrated the interesting potential of these type of ligand with heteroatoms groups as CPE modifiers, since it entraps target analytes over its surface through hydrogen bonding or other electrostatic interactions and enhancement the electrochemical signal [20-22]. To the best of our knowledge, the electrochemical sensing of scopolamine as food contaminant with MS-CPEs has not been reported.

In the current work, firstly three MSs (MSU-2, HMS and SBA-15) were synthesized and functionalized with a 2-mercaptopyrimidine (MPY)-derivative and evaluated to develop MS-CPEs. The influence of the silica type on the electrochemical behavior of the MS-CPEs was studied by cyclic voltammetry (CV) and differential pulse voltammetry (DPV), using potassium ferrocyanide and scopolamine as probes. In a next step, parameters controlling the performance of the CPE modified with the functionalized MS (electrolyte support, pH, accumulation time) were optimized for scopolamine determination by DPV. Finally, using electrochemical sensor developed with HMS-MPY as the best, characteristics such as reproducibility, stability, selectivity and sensibility were evaluated. The capability of the HMS-MPY-CPE was investigated for a rapid determination of scopolamine in tea and herbal tea infusions.

2. Experimental

2.1. Reagents and materials

For MSs preparation, tetraethylorthosilicate (TEOS, 98 %), Tergitol® NP-9, poly(ethylene glycol)-block-poly(propylene glycol)-blockpolyethylene glycol (Pluronic 123), N,N-dimethyldodecylamine (DDA, 98 %), 2-mercaptopyrimidine (MPY, 98%), 3-chloropropyl triethoxysilane (CPTS, 95 %), sodium fluoride (95 %) and dimethylformamide (DMF, 99 %) were purchased from Sigma–Aldrich (St. Louis, MO, USA). Trimethylamine (TEA, 99 %) was obtained from Acros Organics (Geel, Belgium). Chlorhydric acid (37 %), toluene, diethyl ether and ethanol absolute were purchased from Scharlab (Barcelona, Spain).

For MS-CPEs preparation and electrochemical studies, scopolamine hydrobromide (98 %), atropine sulfate (99 %), quercetin (95 %), gallic acid (97.5-102.5 %), sodium tetraborate and mineral oil were obtained from Sigma-Aldrich. Sodium phosphate (99-102 %), sodium sulfate (99 %), calcium nitrate (99-103 %), potassium chloride (99.5 %) and magnesium sulfate (98 %), all of them of analytical grade, were obtained from Panreac (Castellar del Valles, Spain). Potassium ferrocyanide trihydrate (99 %) was purchased from Across Organics. Graphite powder was obtained from Sugelabor (Madrid, Spain). Ultrapure water (resistivity 18.2 MΩ cm) used in the preparation of solutions was obtained from a Millipore Milli-Q-System (Waters, USA).

Scopolamine was dissolved in Milli-Q water to prepare a 0.005 M standard solution and stored at 4 ºC. For electrochemical studies, a working solution of scopolamine (5 μM) was prepared daily by diluting the standard solutions with the corresponding electrolyte. For linearity determination, working solutions of scopolamine

from 0.5 to 200 μM were prepared directly in the electrochemical cell by adding successive aliquots of scopolamine 0.005 M.

2.2. Synthesis of MSs

MSU-2 was prepared according to Pérez-Quintanilla et al. [23]. Concisely, TEOS was added to a stirred 0.08 M solution of Tergitol® NP-9 in Milli-Q water to obtain a milky suspension, which was later aged without agitation for 20 h. In the second step, a 0.24 M sodium fluoride solution was added drop wise with stirring to obtain NaF/TEOS molar ratio 0.025:1. The solution was placed in a bath with agitation at 55 ºC for 48 h. The obtained product was filtered off, washed with Milli-Q water, dried and calcined in air at 600 ºC for 12 h.

HMS was synthesized following the method described by Pérez-Quintanilla et al. [24]. Briefly, 3 g of DDA were dissolved in 13 mL of Milli-Q water and 7.6 mL of ethanol. The solution was stirred until its homogenization, and subsequently 4.2 g of TEOS were added drop by drop. The solution was stirred for 18 h, yielding a thick white suspension that was filtered and dried at 80 ºC for 1 h. The amine was removed by heating the solid at reflux in ethanol with a Soxhlet for 8 h. Finally, the rests of surfactant were removed by calcination at 550 ºC for 18 h.

SBA-15 was prepared according to the method of Zhao et al. [25] as follows: 2.42 g of Pluronic 123 were dissolved in 72 g of 2 M HCl solution and 18 mL of Milli-Q water with stirring at 35 ºC. Then, 5.1 g of TEOS were slowly added, and the resulting mixture was stirred at the same temperature for 20 h. After this reaction time, the stirring was stopped and the temperature was increased to 80 ºC and maintained for 24 h. The solid

product was recovered by filtration and washed with water. Then, it was calcined at 500 ºC for 18 h.

2.3. Synthesis of 2-mercapropyrimidine derivative and functionalization of MSs

MPY-derivative was prepared according to the method of Pérez-Quintanilla et al. [26]. Briefly, 5.00 g of MPY (44 mmol) was immersed in 50 mL of DMF. CPTS and TEA were then added in a 1:2:1 stoichiometry (MPY:CPTS:TEA). The mixture was heated for 48 h at 115 ºC with magnetic stirring under a nitrogen atmosphere using standard Schlenk-tube techniques. The mixture was allowed to cool, the solvent was evaporated and the resulting product was extracted with hexane (2 × 30 mL). The hexane was evaporated and the excess CPTS was distilled under vacuum (150 ºC and 0.75 mm Hg). The resulting viscous oil (dark-orange colour, yield 96 %) was characterized by ^{1}H NMR spectroscopy (Fig. SM1, supplementary information).

1.5 g of activated MS (12 h at 150 ºC under high vacuum) was reacted with 1.5 mL MPY-derivative in dry toluene for 24 h at 80 ºC under N_2 atmosphere. The resulting mesostructured silicas (MSU-2-MPY, HMS-MPY and SBA-15-MPY) were filtered off and washed with toluene, ethanol and diethyl ether.

2.4. Characterization of bare and functionalized MSs

For MS characterization, N_2 gas adsorption-desorption isotherms were recorded using a Micrometrics ASAP 2020 analyzer. The surface specific area was calculated by Brunauer-Emmett-Teller (BET) method and the pore size distribution was obtained using Baret-Joyner-Halenda (BJH) model on the desorption branch. X-ray diffraction (XRD)

patterns of the silicas were obtained on a Philips diffractometer model PW3040/00 X'Pert MPD/MRD at 45 KV and 40 mA, using Cu-Kα radiation (λ= 1.5418 Å). Scanning electron micrographs (SEM) were obtained on a XL30 ESEM Philips microscope with an energy dispersive spectrometry system. The samples were treated with a sputtering method with the following parameters: sputter time 100 s, sputter current 30 mA, and film thickness 20 nm using sputter coater BAL-TEC SCD 005. Conventional transmission electron microscopy (TEM) was carried out with a TECNAI 20 Philips electros microscope operating at 200 kV, with a resolution of 0.27 nm and ± 70 º of sample inclination, using a BeO sample holder. ^{29}Si cross-polarisation magic angle spinning nuclear magnetic resonance (CP MAS-NMR) spectra were recorded on a Varian-Infinity Plus 400 MHz Spectrometer operating at 79.44 MHz proton frequency. ^{13}C CP MAS-NMR spectra were recorded on a Bruker Avance III/HD 9.4 Teslas Spectrometer operating at 400 MHz proton frequency. Elemental analysis (% C, N and S) was performed with a Flash 2000 Thermo Fisher Scientific Inc. analyzer.

2.5. Preparation of MS-CPEs

The modified CPEs were prepared by mixing 0.100 g (20 % w/w) of bare or functionalized MSs with 0.300 g (60 % w/w) of carbon paste and 0.100 g (20 % w/w) of mineral oil, until obtaining a homogeneous carbon paste, according to a previous work [21]. Then, a portion of the paste was packed firmly into the end of a 5.0 cm long polyethylene tube (3 mm i.d. having 3 mm depth), with a metallic wire as inner electrical contact. Smoothing of the electrode surface was made by hand-polishing on a filter paper. When necessary, a new electrode surface was achieved by a simple polishing. By replacing the wetted paste by freshly prepared uniform paste (and polishing them again

on a filter paper) a new working electrode was obtained. For comparative analysis unmodified CPE was prepared and applied in the same way. All freshly-made electrodes were activated by performing 10 cycles of CV in 0.1 M phosphate buffer (pH 8) until the background was stable. This activation process was carried out each day prior to use the electrodes.

2.6. Voltammetric measurements

For electrochemical studies with MS-CPEs, CV and DPV measurements were performed on a hand-held, battery-powered bipotentiostat (μSTAT200, Dropsens) using a conventional voltammetry cell (volume of the cell 25 mL) equipped with three electrodes: a MS-CPE as working electrode, a saturated Ag/AgCl as reference electrode and a platinum wire as auxiliary electrode. A PC with DropView software for Windows was used to control the instrument, plot the measurements and perform the analysis of results.

To study the behaviour of electrochemical reaction at the electrode surface with potassium ferrocyanide as redox probe (1 mM), 0.1 M phosphate buffer (pH 8.0) was used as supporting electrolyte and cyclic voltammograms were recorded by applying a potential range from -1.0 to +1.5 V at different scan rate.

For scopolamine measurements, unless otherwise stated, a 0.1 M phosphate buffer (pH 8.0) was used as electrolyte support. Cyclic voltammograms were recorded from 0.0 to +1.5 V at different scan rate. Under optimized conditions, differential pulse voltammograms were recorded from 0.0 to +1.4 V, after open-circuit accumulation of scopolamine for 1 min, with stirring at 200 rpm. The pulse amplitude was 10 mV with a potential step height of 5 mV, the pulse width was 40 ms and the scan rate was 100 $mV \cdot s^{-}$

[1]. After each measurement, to ensure that scopolamine was not present on the electrode surface, regeneration of the electrode surface was performed by 2–3 DPV measurements in 0.1 M phosphate buffer (pH 8). Each measurement was performed in triplicate and the average value was reported. All measurements were carried out at room temperature.

2.7. Sample analysis

Five samples of teas and herbal teas (green tea, red tea, rooibos tea, chamomile tea and fennel tea) commercialized in local supermarkets of Madrid (Spain) were analyzed. Tea and herbal tea samples were stored unopened in a dry and dark compartment at room temperature until analysis. Infusions were prepared according manufacturer recommendation as follows: one bag (1.5 g) of each sample was placed in a porcelain cup and 200 mL of boiling Milli-Q water was poured on it, the cap was covered allowing brewing for 3 min and then the bag was removed from the infusion. For teas and herbal tea infusions analysis, not sample pretreatment was need. Typically, 23 mL phosphate buffer 0.1 M (pH 8) was transferred to the electrolytic cell and 2 mL of the infusion (at room temperature) were added. Then, differential pulse voltammograms were recorded under the optimal experimental conditions and the results were obtained.

3. Results and discussion

3.1. Characterization of MSs

The N_2 adsorption-desorption isotherms and pore size distribution for MSs are shown in Fig. 1A. For these materials, the isotherms are type IV according to the

I.U.P.A.C. classification and have a hysteresis loop that is representative of framework-confined mesoporosity. In SBA-15, HMS and MSU-2, the volume of nitrogen adsorbed increased at a relative pressure (P/P_0) of approximately 0.14, 0.15 and 0.30, respectively, what represents capillary condensation of nitrogen within the mesopore structure. The inflection position shifted slightly toward lower relative pressures (0.14, 0.13 and 0.14), the volume of N_2 adsorbed decreased and the hysteresis loop decreased with functionalization.The physicochemical properties of the MSs such as the Brunauer-Emmett-Teller surface area (S_{BET}), the total pore volume, and the Barrett, Joyner and Halenda (BJH) average pore diameter are shown in Table 1. SBA-15, HMS and MSU-2 possessed very high S_{BET}, with typical pore volume and average BJH pore diameter values for surfactant-assembled mesostructures [25]. HMS was the material with the highest S_{BET}, but with a small pore diameter (1078 $m^2 \cdot g^{-1}$ and 25 Å, respectively), while SBA-15 was the material with the lowest S_{BET} and the highest pore diameter (780 $m^2 \cdot g^{-1}$ and 64 Å, respectively). As it can be seen in Table 1, after functionalization, a decrease in the $S_{BET,}$ pore volume and average BJH pore diameter was observed in all cases that can be interpreted because MPY groups are present on the silica surface.

Fig. 1C shows XRD patterns of bare and functionalized MSs. These materials exhibit a well-resolved XRD pattern at low 2θ values with a narrow (100) diffraction peak, below 5 º, indicating a mesoscopic order system in the silicas. HMS and MSU-2 exhibit a single (100) diffraction peak at 2.42 º and 1.92 º, respectively. These XRD patterns are typical of materials with uniform pores in the mesoporous range and non-symmetrical 3D wormhole-like structure of the porous framework. On the other hand, SBA-15 shows a very sharp (100) diffraction peak around 1.03 º and two additional weak high order peaks (110 and 200) around 1.94 º and 2.66 º, respectively. XRD pattern of SBA-15 suggest a significant degree of long range ordering of the structure and well-

formed hexagonal pore arrays. The decrease in the (100) XRD diffraction peak for SBA-15-MPY, HMS-MPY and MSU-2-MPY provides further evidence of grafting occurring inside the mesopore channels, since the attachment of organic functional groups in the mesopore channels tends to reduce the scattering power of the mesoporous silicate wall. The XRD pattern of the functionalized silicas also suggest that the structural order of the synthesized materials is maintained after functionalization.

The wall thickness can been estimated considering the (100) interplanar distance and the pore diameter, by using Equation (1) for SBA-15 and Equation (2) for HMS and MSU-2. Table 1 shows the values of wall thickness obtained for each silica. SBA-15 have the higher wall thickness value (31.5 Å), more than twice the value obtained for the 3D wormhole materials (HMS and MSU-2). In functionalized MS, an increase in the wall thickness was observed, that can be attributed to the presence of MPY groups inside the mesopores.

$$Wall\ thickness = \frac{2d_{100}}{\sqrt{3}} - BJH\ average\ pore\ diameter \qquad (1)$$

$$Wall\ thickness = d_{100} - BHJ\ average\ pore\ diameter \qquad (2)$$

Evidence for disordered structure of HMS and MSU-2 was confirmed by TEM. These micrographs (Fig. 2) showed irregularly aligned mesopores throughout the materials with relatively uniform pore sizes (wormhole-like pore arrangement). On the other hand, TEM images of SBA-15 (Fig. 2) demonstrated a clear arrangement of ordered hexagonal pores with uniform size throughout the structure. SEM pictures demonstrated the spherical or pseudo-spherical morphology of HMS and MSU-2 particles, while for SBA-15 the particle morphology was rod-like.

The amount of attached molecules onto the MS surface was calculated from the percentage of sulphur in the functionalized silicas, estimated by elemental analysis (Table 1). The functionalization degree (L_0) obtained in MSU-2-MPY was the highest (0.94 $mmol \cdot g^{-1}$), whereas for SBA-15-MPY the lowest L_0 value was observed (0.70 $mmol \cdot g^{-1}$).

The successful incorporation of MPY ligand in functionalized HMS was additionally confirmed by ^{29}Si CP MAS-NMR and ^{13}C CP MAS-NMR spectroscopy. The ^{29}Si CP MAS-NMR spectrum in the solid state for HMS-MPY confirmed the covalent bond formed between the MPY groups and the silanol groups dispersed on the HMS surface (Fig SM2a, supplementary information). HMS-MPY showed three main peaks at -112, -105 and -95(*sh*) ppm which were assigned to Q^4 framework silica sites ($(SiO)_4\boldsymbol{Si}$), Q^3 $(SiO)_3\boldsymbol{Si}OH$) and $Q^2(SiO)_2\boldsymbol{Si}(OH)_2$) silanol sites, respectively. In addition, this spectrum showed two other peaks at -63 and -53 ppm, which are assigned to T^2 ($(SiO)_2\boldsymbol{Si}$OH-R) and T^3 ($(SiO)_3\boldsymbol{Si}$-R) sites, respectively. ^{13}C CP MAS-NMR spectra (Fig SM2b) provide important features related to the immobilization of functional groups on the inorganic structure of the material prepared. The carbon atoms corresponded to the ligand ring, designated as (3), (4) and (5), gave signals at 8.99, 21.36 and 31.62 ppm, respectively. The signal due to methylene (2) of the ethoxy group appears at 56.92 ppm and the signal of the methyl group (1) at 15.14 ppm. The aromatic carbons numerated (6), (7), (8) and (9) were assigned to signals at 171.52, 155.90, 115.05 and 155.90 ppm, respectively.

3.2. Electrochemical studies of $[Fe(CN)_6]^{3-/4-}$ on MS-CPEs

In the initial studies, the electrochemical behavior of $[Fe(CN)_6]^{3-/4-}$ redox ions using the MS-CPEs was investigated by CV. Fig. 3 displays the CV profiles (scan rate

100 $mV \cdot s^{-1}$) of unmodified (graphite) and modified (with bare or functionalized MSs) CPEs obtained with 1 mM $K_4[Fe(CN)_6]$ solution in 0.1 M phosphate buffer (pH 8). As can be seen, for graphite and bare silica-modified CPE the voltammograms showed a pair of low-intensity redox peaks with very large difference (ΔE_p) between cathodic (E_{pc}) and anodic (E_{pa}) peak potentials (ΔE_p = 1.16 V for graphite and ΔE_p between 0.83-0.87 V for bare silica modified-CPEs). On the other hand, all the CPEs modified with the functionalized materials showed better electrochemical response, and these voltammograms showed a pair of well-defined and more prominent quasi-reversible redox peaks (ΔE_p = 0.59, 0.57 and 0.40 V for SBA-15-MPY, HMS-MPY and MSU-2-MPY, respectively) indicating faster electron transfer kinetics at the electrode interface. In addition, the anodic peak current/cathodic peak current ratio (I_{pa}/I_{pc}) was very close to 1 (0.90 for SBA-15-MPY and 0.93 for HMS-MPY and MSU-2-MPY), confirming the quasi-reversibility of the system. The SBA-15-MPY material showed the lower reversibility, because it presented the I_{pa}/I_{pc} less closed to 1 and the higher ΔE_p value. This fact can be attributed to the large pore wall thickness of SBA-15-MPY in relation to the other materials (Table 1), which could increase the resistance for electron transfer [27].

In order to evaluate the electrochemical process in the interface electrode solution, the effect of scan rate was studied (from 10 to 200 $mV \cdot s^{-1}$). Fig. 4 shows the cyclic voltammograms obtained for CPEs modified with the functionalized silicas, with 1 mM $K_4[Fe(CN)_6]$ solution in 0.1 M phosphate buffer. The inset figures show that there is a linear relationship between the current peak intensity and the squared root of the scan rate, making evident that the redox reaction at the electrode surface was controlled by diffusion. Therefore, by applying Randles-Sevcik equation (3), the electroactive area of the working electrodes can be calculated as follows [28]:

$$I_{pa} = (2.69 \times 10^5)\, n^{3/2} A D^{1/2} C \nu^{1/2} \quad (3)$$

where I_{pa} is the anodic peak current (A), n is the number of electrons transferred in the redox reaction (n = 1), A is the electroactive area (cm^2), D ($cm^2 \cdot s^{-1}$) is the diffusion coefficient (6 x 10^{-6} for $[Fe(CN)_6]^{3-/4-}$ in aqueous medium [29]), C ($mol \cdot cm^{-3}$) is the concentration and v ($V \cdot s^{-1}$) is the scan rate. Compared with the geometric surface area of the working electrode (0.07 cm^2), the values of A calculated for the CPEs modified with the functionalized silicas were significantly higher (0.22, 0.27 and 0.26 cm^2 for SBA-15-MPY, HMS-MPY and MSU-2-MPY, respectively). These results agree with previous studies, which indicated that A of MS-CPEs can be 3 or 4 times higher than the geometric surface areas [30]. In addition, these values evidenced that materials with the higher surface areas (HMS-MPY and MSU-2-MPY) showed also the higher A that indicates a better performance of these modified electrodes.

3.3. Electrochemical behavior of scopolamine on MS-CPEs

Preliminary electrochemical measurements by CV were carried out in order to study the general behavior of scopolamine at MS-CPEs. Fig. 5 illustrates cyclic voltammograms (100 $mV \cdot s^{-1}$) of MS-CPEs in 50 μM of scopolamine and phosphate buffer (0.1 M, pH 8) as supporting electrolyte. As can be seen, with bare silica-modified CPEs it was not possible to observe any defined peak for scopolamine, in the assayed experimental conditions. However, in CPE modified with functionalized silicas (HMS-MPY, MSU-2-MPY and SBA-15-MPY) an oxidation peak was observed, indicating that functionalization of MSs played an important role, which made it easier for the transfer of electrons to be taking place, so MPY groups were necessary to improve the sensitivity in the voltammetric determination of this compound. SBA-15-MPY-CPE, which

presented the lowest *A*, showed a poorly defined oxidation peak around + 1.1 V. On the other hand, MSU-2-MPY-CPE and HMS-MPY-CPE exhibited a better-defined oxidation peak at 1.08 and 1.13 V, respectively. On the reverse scan, no reduction peak was observed revealing that the electrode process of scopolamine is an irreversible charge-transfer process.

Fig. 6 shows cyclic voltammograms obtained in functionalized-silica CPEs electrodes varying the scan rate from 10 to 100 $mV \cdot s^{-1}$, using 50 μM of scopolamine in 0.1 M of phosphate buffer (pH 8). As can be seen, increasing the scan rate the oxidation peak current increased and the peak potential shifted to higher potential values. A linear relationship between the peak current and the square root of the scan rate was obtained in HMS-MPY-CPE and MSU-2-MPY-CPE, which indicates a diffusion-controlled redox process for scopolamine oxidation [31]. A linear correlation between Log I_{pa} (μA) and Log v ($mV \cdot s^{-1}$) was also observed for both CPEs (Log I_{pa} = 0.567 Log v – 0.545, R^2= 0.999, and Log I_{pa} = 0.7456 Log v – 0.7599, R^2= 0.959, for HMS-MPY-CPE and MSU-2-MPY-CPE, respectively), indicating that the peak current is controlled by both charge transfer and mass transport. Taking into account that the theoretical value expected for an ideal reaction of organic molecules in solution (purely diffusion-controlled process) is close to 0.5, whereas for adsorption-controlled process is close to 1.0 [32], it can be noted that the slopes obtained with these CPEs (between 0.5 and 1.0) suggest diffusion and adsorption joint control. On the other hand, non-linear correlation was observed in SBA-15-MPY-CPE, over the whole range of the scan rate studied.

In addition, for HMS-MPY-CPE, a linear relationship between E_{pa} (V) and Log v ($mV \cdot s^{-1}$) was observed with the following equation: E_{pa} = 0.0316 Log v + 1.0563 (R^2= 0.991) and this behavior was consistent with the nature of the reaction in which the electrode reaction is coupled with and irreversible follow-up chemical step. The number

of electrons involved in the oxidation could be estimated from the slope of E_{pa} *vs*. Log *v* (Ep_a/Log *v*) using the following equation [31]: Ep_a/Log *v* = 30 mV/ nα, where n is the number of electrons transferred and α is assumed to be 0.5 for organic molecules with irreversible electrode processes. The n value estimated was 1.898, indicating that two electron per molecule are involved in the oxidation of scopolamine. Hence, based on these results and according to others works for similar compounds [33-35] the proposed oxidation mechanism of scopolamine is shown in Scheme SM1.

3.4. Electrochemical detection of scopolamine on MS-CPEs by DPV

DPV was evaluated for electrochemical detection of scopolamine on the MS-CPEs and experimental conditions (electrolyte support, pH and accumulation time) were optimized. Firstly, two supporting electrolytes were investigated: 0.1M phosphate buffer and 0.1 M borate buffer (pH in the range from 6.5 to 10.5). Results showed that the oxidation peak current was higher employing phosphate buffer and, as it can be seen in Fig. 7a, the maximum current response was obtained at pH 8, showing in these conditions a low background current and a well-defined oxidation peak. The pK_a of scopolamine is reported to be 7.75 within literature [36], which is similar to the pH value for the best response that is in accordance with the mechanism of scopolamine electrochemical reaction proposed in Scheme SM1. Therefore, this electrolyte and pH value was chosen for subsequent analytical experiments, for considering the sensitive determination of scopolamine.

Accumulation is generally an effective way to enhance the sensitivity on the voltammetry analysis, so experiments were carried out in order to evaluate if immersion of the working electrode in a scopolamine solution could improve the adsorption process

on the MS-CPEs surface. The influence of the accumulation time (in open circuit conditions) on the peak current was evaluated from 0 to 5 min (scan rate 100 $mV \cdot s^{-1}$) and the corresponding current was measured using 5 μM scopolamine in a 0.1 mM phosphate buffer (pH 8). The effect of accumulation time on the peak current of scopolamine is shown in Fig. 7b. In HMS-MPY-CPE and SBA-15-MPY-CPE, the oxidation peak current increased linearly with increasing the accumulation time from 0 to 1 min and from 0 to 2 min, respectively, but with further increasing accumulation time the current response do not increase. This fact presumable indicates that the limiting value of the amount of scopolamine at these electrodes was achieved. On the other hand, in MSU-MPY-CPE not significant peak current increase was observed (between 0 and 1-2 min) and worse reproducibility, with a higher background current, was observed for repeated measurements. It must be noted (Fig. 7b) that under optimized conditions, the maximum peak current value was obtained for HMS-MPY-CPE suggesting that the adsorption process of scopolamine on this electrode was more effective.

In order to develop a voltammetric method for determination of scopolamine, more sensitive DPV mode was selected as the detection method, since the anodic peak obtained was better-defined and higher than those obtained by CV mode. Thus, after optimization of experimental conditions, the relationship between the oxidation peak current and the scopolamine concentration (C) was examined (Table SM1). It was found that the I_{pa} was proportional to C, over the range 0.9 to 200 μM on the HMS-MPY-CPE, according to the following equation: I_{pa} (μA) = 0.00219 C (μM) + 0.0194 (R^2= 0.9998) as shown Fig. 8. The limit of detection (LOD) and limit of quantification (LOQ), calculated as 3 or 10 times the standard deviation (SD) of five measurements of the peak current of the smallest concentration of the calibration plots divided by the slope of the calibration plots [32], were found to be 0.3 μM and 0.9 μM, respectively. On the MSU-

2-MPY-CPE and SBA-15-MPY-CPE lower linear ranges (LR) and higher LOD and LOQ were observed, with the following calibration plots: I_{pa} (μA) = 0.0014 C (μM) - 0.0033 (R^2= 0.9999) and I_{pa} (μA) = 0.0014 C (μM) - 0.0033 (R^2= 0.9996), respectively. In view of these results, subsequent studies (repeatability, reproducibility, stability, interferences and sample application) were only carried out with the HMS-MPY-CPE.

A comparison of LODs and LR of the HMS-MPY-CPE with other reported electrochemical assay of scopolamine based on conventional modified electrodes were summarized in Table 2. As can be seen, LOD of the reported method is low or comparable with those obtained by other methods.

3.5. Repeatability, reproducibility and stability of HMS-MPY-CPE

Repeatability, reproducibility and stability are important parameters for the evaluation of the performance of an electrode for its practical applications. Firstly, the current response on HMS-MPY-CPE after six successive measurements of 5 μM scopolamine by DPV (in the optimal conditions) were compared, in order to evaluate the repeatability of the electrode. Relative standard deviation (RSD, %) values lower than 4 % were achieved, pointing to the excellent repeatability of HMS-MPY-CPE. In addition, the current response was higher than 90 % from the initial value after 70 measures carried out in four consecutive days. To study the reproducibility of the HMS-MPY-CPE, three different electrode surfaces were used in different days and differential pulse voltammogram responses of 5 μM scopolamine solution were recorded, with a RSD of 8 %. The stability of the electrode was tested by storing the paste (mixture of silica/carbon paste/mineral oil, 20/60/20, w/w/w) at 25 ºC for 5 weeks and 95 % current responses from the initial values were retained. The results revealed good repeatability, reproducibility

and long-term stability of the developed sensor, which could be attributed to the mesoporous framework stability of the HMS material.

3.6. Interferences studies and samples analysis

The selectivity of the developed sensor was evaluated in the presence of various common interfering compounds found in tea and herbal tea infusion samples according with the literature [38]. Table 3 shows the variation of peak current response of scopolamine (10 μM) in the presence of some phenolic compounds commonly found in tea samples (quercetin and gallic acid, 50 μM), alkaloids (caffeine and atropine, 250 μM) and inorganic ions (Na^+, K^+ and Mg^{2+}, 1000 μM), all of them on excess concentration. As can be seen, the presence of quercetin, gallic acid, Na^+ and K^+ did not produced or produced only negligible change (below 15 %) in the peak current of scopolamine. 1000-fold Mg^{2+} (concentration twice higher than usually found in teas) caused a significant increase in the scopolamine peak current, being able to interfere with its determination. However, it is worth noting that an excess of atropine, tropane alkaloid usually found together with scopolamine, did not interfered with its oxidation signal. Based on the results obtained, the sensor developed showed good enough selectivity, but for quantitative purposes, the standard addition method can be used in order to avoid the matrix effects.

Finally, in order to evaluate the performance of the developed HMS-MPY-CPE by practical analytical applications, the determination of scopolamine was carried out in tea (red, green and rooibos tea) and herbal tea (chamomile and fennel tea) infusion samples. Two milliliters of each infusion was added into 23 mL 0.1 M phosphate buffer,

pH 8 (12.5 times dilution) and DPV was recorded under the optimal experimental conditions. The scopolamine concentration was determined by the standard addition method to compensate the matrix effect from the infusion samples (Fig. 9). Taking into account that the therapeutic dose than cause physiological effects is around 180 μM [39, 40], scopolamine was added to the samples for recovery test to achieve a final concentration (in the cell) of 10 μM. This demonstrate that the sample dilution in the cell would not impair the applicability of the developed method. As it can be seen in Table 4, good correlations between amount added and determined were obtained (recoveries between 83 ± 5 and 101 ± 1 %), indicating that the sensor can be effectively employed to attain acceptable results for determination of scopolamine in tea and herbal tea infusion samples.

4. Conclusions

In this work, an electrochemical method for the rapid control of scopolamine has been developed. Mesostructured silicas (MSU-2, HMS, SBA-15) were successfully synthesized, functionalized with 2-mercaptopyrimidine groups, characterized and used to prepare modified CPEs for the detection of scopolamine. The electrochemical response of scopolamine showed great difference by the presence of MPY groups on the silica surface. CPE modified with HMS-MPY produced a well-defined and sensitive oxidation peak for the analyte in DPV. This sensor displayed wide linear range, low detection limit, good reproducibility and long time stability. The DPV method developed with the HMS-MPY-CPE provided reliable results using the standard addition method for determination of scopolamine in tea and herbal tea infusions without sample treatment.

Acknowledgments

Authors thank financial support to MCIU/AEI/FEDER, UE (RTI2018-094558-B-100, EVALKALIM).

Appendix A. Supplementary data

Supplementary data to this article can be found online

References

[1] P. Adamse, H.P. Van Egmond, Tropane alkaloids in food, RIKILT Report, 2010.011 (2010) 1-24. http://edepot.wur.nl/160741

[2] EFSA (2013) Scientific opinion on tropane alkaloids in food and feed. EFSA panel of contaminants in the food chain, EFSA Journal, 11: 3386-3499. https://doi.org/10.2903/j.efsa.2013.3386

[3] B.P. Gaire, L. Subedi, A review on the pharmacological and toxicological aspects of Datura stramonium L., J. Integr. Med. 11 (2013) 73-79. https://doi.org/10.3736/jintegrmed2013016

[4] Commission recommendation (EU) 2015/976 (2015) Commission recommendation of 19 June 2015 on the monitoring of the presence of tropane alkaloids in food, Official Journal of the European Union, L157 (2015) 97-98.

[5] E. Aehle, B. Dräger, Tropane alkaloids analysis by chromatography and electrophoresis techniques: An update, J. Chromatogr. B 878 (2010) 1391-1406. http://doi:10.1016/j.jchromb.2010.03.007

[6] A. Caligiani, G. Palla, F. Bonzanini, A. Bianchi, R. Bruni, A validated GC-MS method for the detection of tropane alkaloids in buckwheat (FagopyronesculentumL.) fruits,

flours and commercial foods, Food Chem. 127 (2011) 204–209. https://doi.org/10.1016/j.foodchem.2010.11.141

[7] H.G.J. Mol, R.C.J. Van Dam, P. Zomer, P.P.J. Mulder, Screening of plants toxins in food, feed and botanical using full-scan high-resolution (Orbitrap) mass spectrometry, Food Addit. Contam. A, 28 (2011) 1405-1423. http://doi:10.1080/19440049.2011.603704

[8] P.P.J. Mulder, M. de Nijs, M. Castellari, M. Hortos, S. MacDonald, C. Crews, J. Hajslova, M. Stranska, Occurrence of Tropane Alkaloids in Food. EFSA Support. Publ. 13:EN (2016) 1140. https://doi.org/10.2903/sp.efsa.2016.EN-1140

[9] A. Romera-Torres, R. Romero-González, J.L. Martínez Vidal, A. Garrido Frenich, Simultaneous analysis of tropane alkaloids in teas and herbal teas by liquid chromatography coupled to high-resolution mass spectrometry (Orbitrap), J. Sep. Sci. 41(2018) 1938-1946. https://doi.org/10.1002/jssc.201701485.

[10] A. Galuszka, Z. Migaszewski, J. Namiesnik, The 12 principles of green analytical chemistry and the significance mnemonic of green analytical practices, TrAC Trend Anal. Chem. 50 (2013) 78-84. https://doi.org/10.1016/j.trac.2013.04.010

[11] S.B. Santos, C.F. Valezi, J. Seremin, C.A.R. Salamanca-Neto, L.H. Dall´Antonia, E.R. Sartori, A simple square-wave voltammetric method for the determination of scopolamine in pharmaceuticals using a boron-doped diamond electrode, Quim. Nova 37 (2014) 1579-1583. http://dx.doi.org/10.5935/0100-4042.20140278

[12] K. Farhadi, A. Karimpour, Electrochemical Behavior and Determination of Hyoscine-N-Butylbromide from Pharmaceutical Preparations, J. Chin. Chem. Soc. 54 (2007) 165-172. https://doi.org/10.1002/jccs.200700026

[13] T. da Costa Oliveira, M.H.P. Santana, C.E. Banks, R.A. Abarza Munoz, E.M. Richter, Electrochemical portable method for on-site screening of scopolamine in

beverage and urine samples, Electroanal. 31 (2019) 567-574. https://doi.org/10.1002/elan.201800707

[14] A. Walcarius, Electroanalysis with Pure, Chemically Modified and Sol-Gel-Derived Silica-Based Materials, Electroanal. 13 (2001) 701-718. https://doi.org/10.1002/1521-4109(200105)13:8/9<701::AID-ELAN701>3.0.CO;2-6

[15] A. Walcarius, Mesoporous materials an electrochemistry, Chem. Soc. Rev. 42 (2013) 4098-4140. https://doi.org/10.1039/C2CS35322A

[16] S. Morante-Zarecero, D. Pérez-Quintanilla, J. Gañán, I. Sierra, A simple and sensitive portable system for a rapid evaluation of Bisphenol A contamination in potable and environmental waters using a mesoporous silica-modified carbon paste electrode, Int. J. Environ. An. Ch. 99 (2019) 607-620. https://doi.org/10.1080/03067319.2019.1609458

[17] M. Silva, S. Morante-Zarcero, D. Pérez-Quintanilla, I. Sierra, Simultaneous determination of pindolol, acebutolol and metoprolol in waters by differential-pulse voltammetry using an efficient sensor based on carbon paste electrode modified with amino-functionalized mesostructured silica, Sensor. Actuat. B-Chem 283 (2019) 434-442. https://doi.org/10.1016/j.snb.2018.12.058

[18] X. Dai, F. Qui, X. Zhou, Y. Long, W. Li, Y. Tu, Amino-functionalized mesoporous silica modified glassy carbon electrode for ultra-trace copper (II) determination, Anal. Chim. Acta 848 (2014) 25-31. https://doi.org/10.1016/j.aca.2014.08.002

[19] A. Sánchez, S. Morante-Zarcero, D. Pérez-Quintanilla, I. del Hierro, I. Sierra, A comparative study on carbon paste electrodes modified with hybrid mesoporous materials for voltammetric analysis of lead (II), J. Electroanal. Chem. 689 (2013) 76-82. https://doi.org/10.1016/j.jelechem.2012.10.026

[20] M. Tiwari, A. Kumar, R. Prakash, Nano-porous network of DMTD-Ag coordination polymer for the ultra trace detection of anticholinergic drug, Polymer 82 (2016) 66-74. https://doi.org/10.1016/j.polymer.2015.11.017

[21] S. Morante-Zarcero, A. Sánchez, M. Fajardo, I. Hierro, I. Sierra, Voltammetric analysis of Pb (II) in natural waters using a carbon paste electrode modified with 5-mercapto-1-methyltetrazole grafted on hexagonal mesoporous silica, Microchim. Act. 169 (2010) 57-64. https://doi.org/10.1007/s00604-009-0287-3

[22] A. Sánchez, S. Morante-Zarcero, D. Pérez-Quintanilla, I. Sierra, I. del Hierro, Determination of Hg (II) in natural waters using a carbon paste electrode modified with hybrid mesostructured silica nanoparticles, Sensor. Actuat. B: Chem. 163 (2012) 38-43. https://doi.org/10.1016/j.snb.2011.12.042

[23] D. Pérez-Quintanilla, A. Sánchez, I. Hierro, M. Fajardo, I. Sierra, Synthesis and Characterization of novel mesoporous silica of the MSU-X family for environmental applications, J. Nanosci. Nanotechnol. 9 (2009) 4901-4909. https://doi.org/10.1166/jnn.2009.1106

[24] D. Pérez-Quintanilla, A. Sánchez, I. del Hierro, M. Fajardo, I. Sierra, Functionalized HMS mesoporous silica as solid phase extractant for Pb(II) prior to its determination by flame atomic absorption spectrometry, J. Sep. Sci. 30 (2007) 1556-1567. https://doi.org/10.1002/jssc.200600540

[25] D. Zhao, Q. Huo, J. Feng, B.F. Chemelka, G.D. Stucky, Nonionic Triblock and Star Diblock Copolymer and Oligomeric Surfactant Syntheses of Highly Ordered, Hydrothermally Stable, Mesoporous Silica Structures, J. Am. Chem. Soc. 120 (1998) 6024-6037. https://doi.org/10.1021/ja974025i

[26] D. Pérez-Quintanilla, I. del Hierro, M. Fajardo, I. Sierra, Adsorption of cadmium(II) from aqueous media onto a mesoporous silica chemically modified with 2-

mercaptopyrimidine, J. Mater. Chem. 16 (2006) 1757–1764. https://doi.org/10.1039/B518157G

[27] L.V. de Souza, D.S. da Rosa, O.S. Tkachenko, A. de Araujo Gomes, T.M.H. Costa, L.T. Arenas, E.V. Benvenutti, The role silica pore structure plays in the performance of modified carbon paste electrodes, Ionics 25 (2019) 3259-3268. https://doi.org/10.1007/s11581-019-02882-0

[28] C. Brett, A.M. Oliveira, Electrochemistry: Principles, Methods, and Applications. Oxford University Press, Oxford, (1993).

[29] R.E. Smith, T.J. Davies, N.B. Baynes, R.J. Nichols, The electrochemical characterization of graphite felts, J. Electroanal. Chem. 747 (2015) 29-38. https://doi.org/10.1016/j.jelechem.2015.03.029

[30] X. Zhang, S. Duan, X. Xu, S. Xu, C. Zhou, Electrochemical behavior and simultaneous determination of dihydroxybenzene isomers at a functionalized SBA-15 mesoporous silica modified carbon paste electrode, Electrochim. Acta 56 (2011) 1951-1987. https://doi.org/10.1016/j.electacta.2010.11.048

[31] A.J. Bard, L.R. Faulkner, Electrochemical method: Fundamentals and applications, 2nd edn. Willey, New York, (2000).

[32] D.K. Gosser, Cyclic Voltammetry. VCH, New York (1994).

[33] R.A. Dar, P.K. Brahman, S. Tiwari, K.S. Pitre, Electrochemical determination of atropine at multi-wall carbon nanotube electrode based on the enhancement effect of sodium dodecyl benzene sulfonate, Colloids Surface. B, 91 (2012) 10-17. https://doi.org/10.1016/j.colsurfb.2011.10.020

[34] H. Bagheri, S.M. Arab, H. Khoshsafar, A. Afkhami, A novel sensor for sensitive determination of atropine based on a Co3O4-reduced graphene oxide modified carbon

paste electrode, New J. Chem. 39 (2015) 3875-3881. https://doi.org/10.1039/C5NJ00133A

[35] S. Mane, R. Narmawala, S. Chatterjee, Selective recognition of atropine in biological fluids and leaves of Datura stramonium employing a carbon nanotube–chitosan film based biosensor, New J. Chem. 42 (2018) 10852-10860. https://doi.org/10.1039/C8NJ01312H

[36] F.J. Muhtadi, M.M.A. Hassan, Analytical profile of scopolamine hydrobromide, Anal. profiles drugs subst. 19 (1990) 477-551. https://doi.org/10.1016/S0099-5428(08)60376-7

[37] H.Y. Aboul-Enein, Electroanalytical methods in pharmaceutical analysis and their validation, Chromatogr. 75 (2012) 811-824. https://doi.org/10.1007/s10337-012-2268-7

[38] A.Y. Yashin, B.V. Nemzer, E. Combet, Y.I. Yashin, Determination of the chemical composition of tea by chromatography methods: A Review, J. Food Research 4 (2015) 56-87. https://doi.org/10.5539/jfr.v4n3p56

[39] K.J. Lusthof, I.J. Bosman, B. Kubat, M.J. Vincenten- van Maanen, Toxicological results in a fatal and two non-fatal cases of scopolamine-facilitated robberies, Forensic Sci. Int. 274 (2017) 79–82. https://doi.org/10.1016/j.forsciint.2017.01.024

[40] E. Le Garff, Y. Delannoy, V. Mesli, V. Hédouin, G. Tournel, Forensic features of a fatal Datura poisoning case during a robbery, Forensic Sci. Int. 261(2016) e17–e21. https://doi.org/10.1016/j.forsciint.2016.02.028

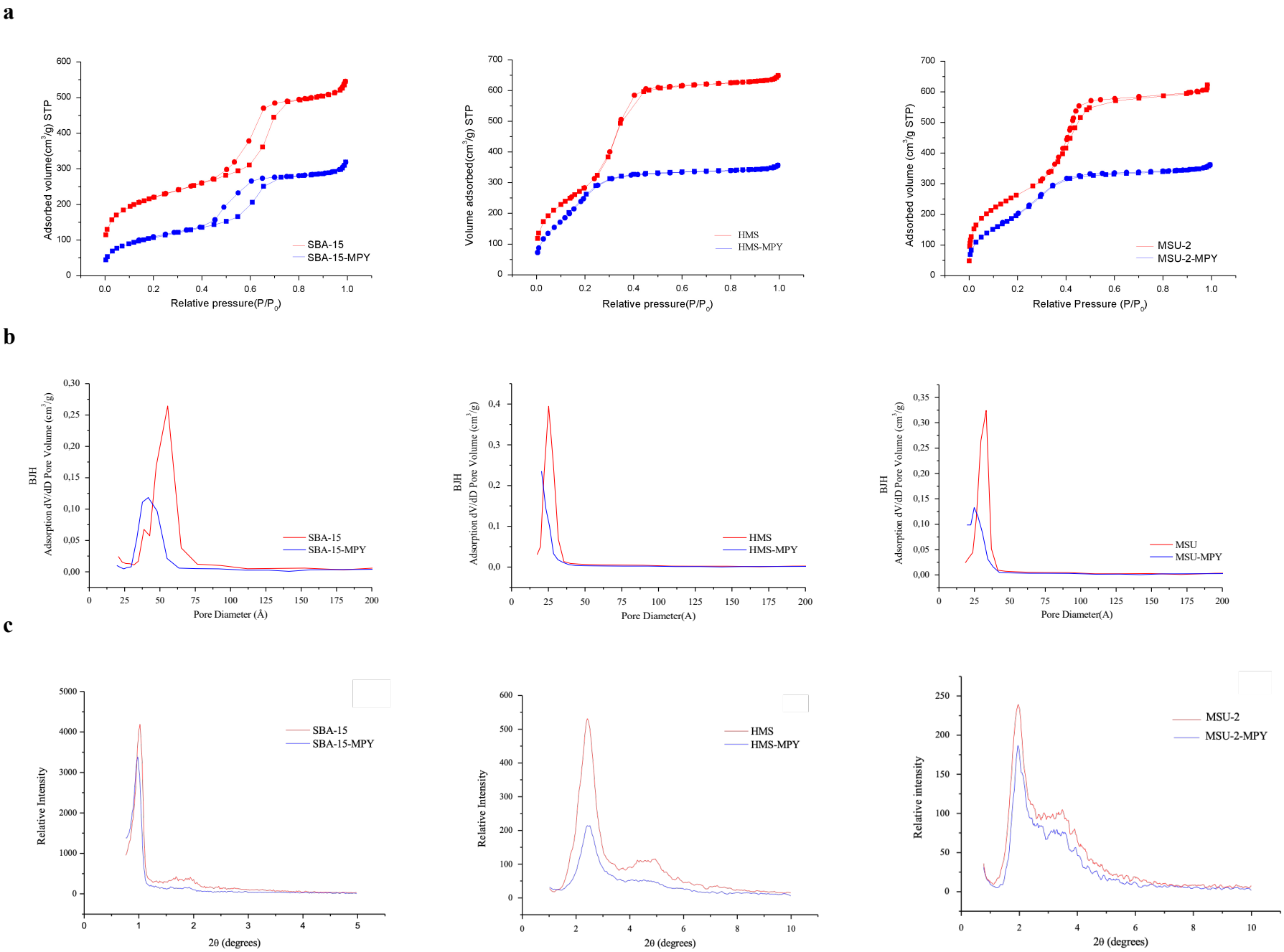

Fig. 1. Characterization of bare and functionalized mesostructured silicas: (a) N2 adsorption-desorption isotherms; (b) pore size distribution; (c) XRD patterns.

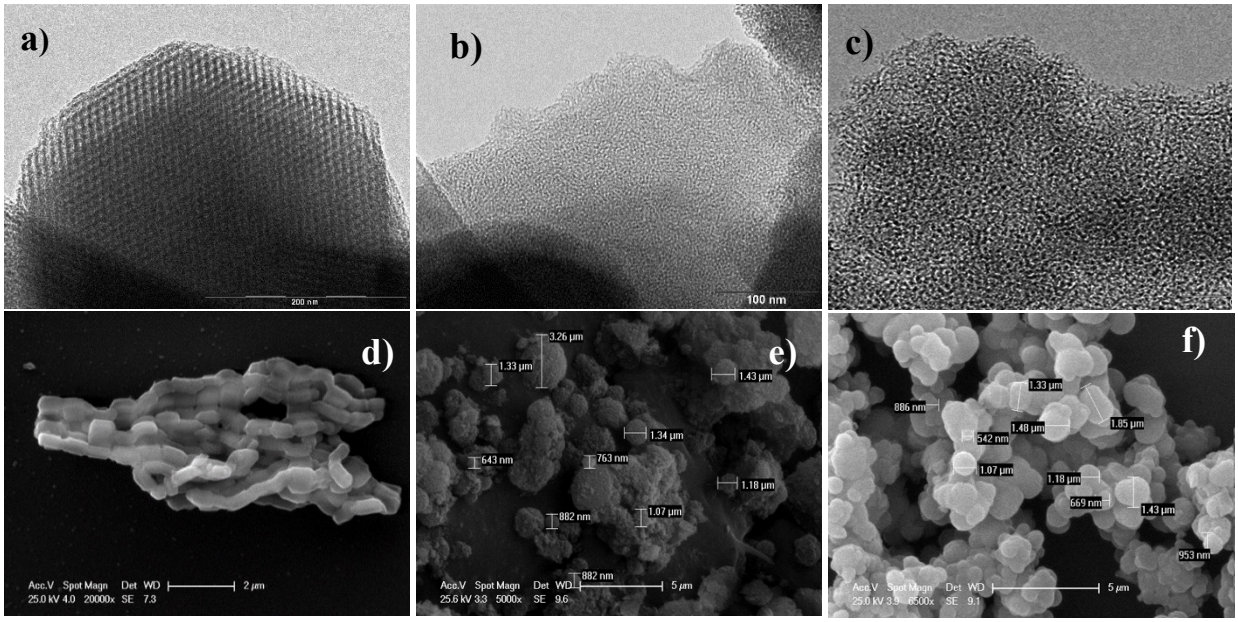

Fig. 2. (a), (b), (c) TEM images of SBA-15, HMS and MSU-2; **(d), (e), (f)** SEM images of SBA-15, HMS and MSU-2.

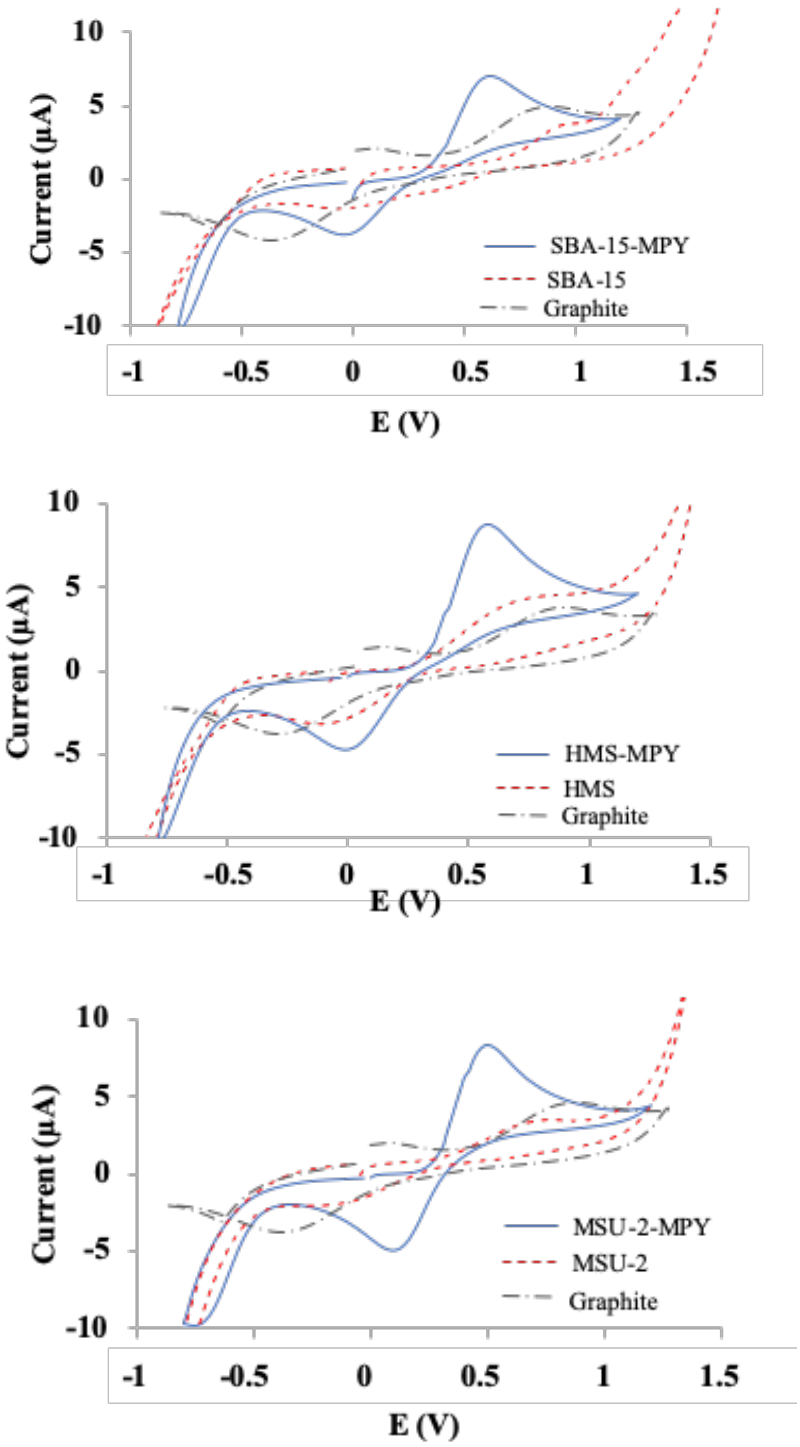

Fig. 3. Cyclic voltammograms of unmodified (graphite) and modified (with bare or functionalized silicas) CPEs in the potential range of – 1 to + 1.5 V obtained with 1 mM $K_4[Fe(CN)_6]$ solution in 0.1 M phosphate buffer (pH 8). Scan rate: 100 $mV \cdot s^{-1}$.

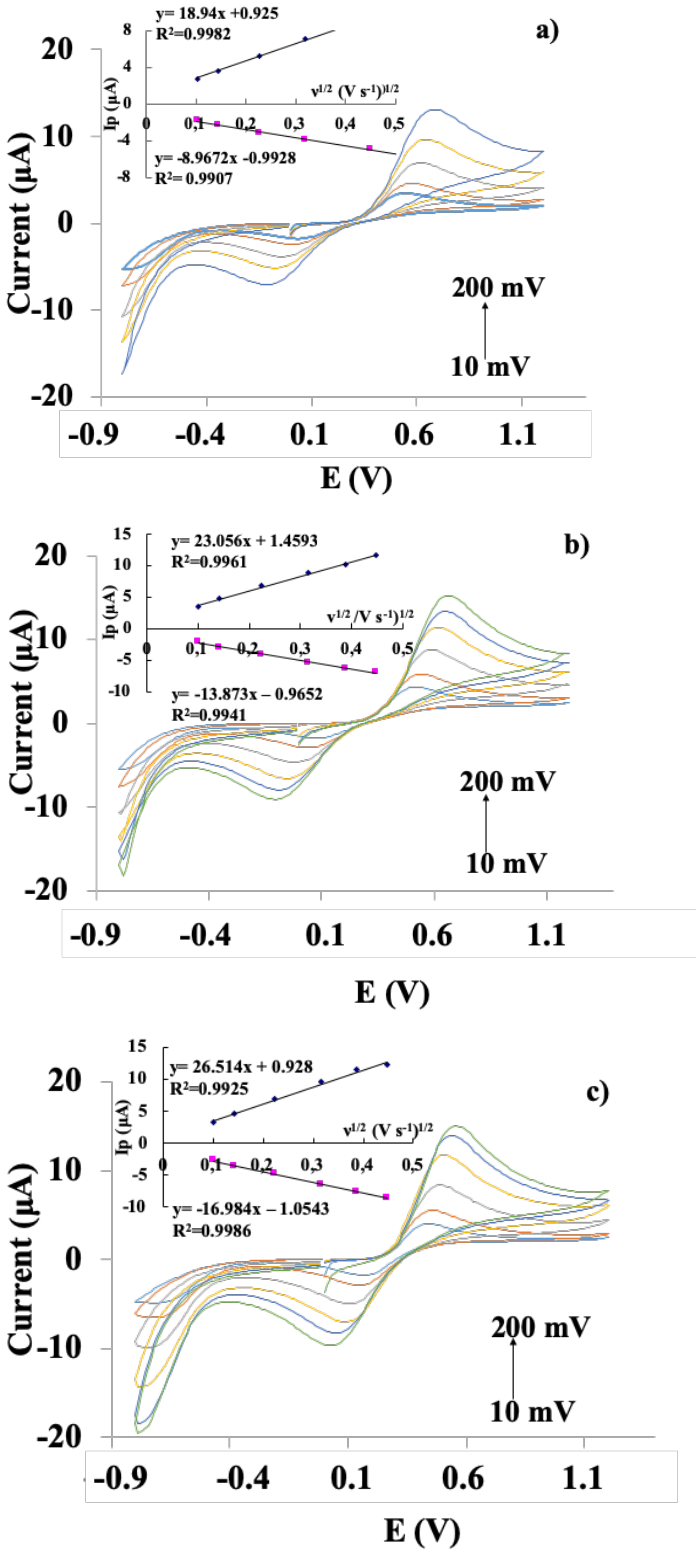

Fig. 4. Cyclic voltammograms of (**a**) SBA-15-MPY, (**b**) HMS-MPY and (**c**) MSU-2-MPY CPEs at different scan rates (10 - 200 $mV \cdot s^{-1}$) performed in 1 mM $K_4[Fe(CN)_6]$ and 0.1 M phosphate buffer (pH 8) supporting electrolyte. Inset shows the linear relationship of the reduction and oxidation peak current (I_p) vs. squared root of scan rate ($\nu^{1/2}$).

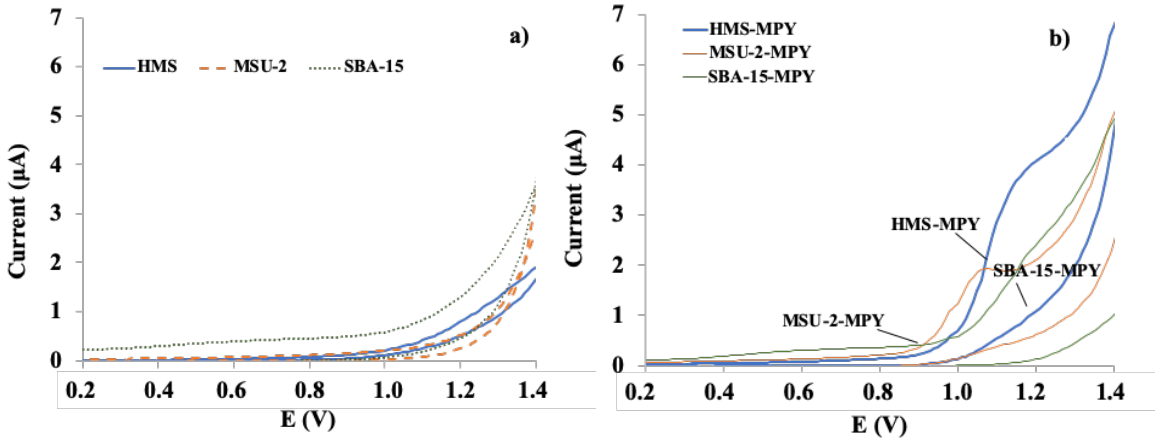

Fig. 5. Cyclic voltammograms of modified CPEs with **(a)** bare silicas and **(b)** functionalized silicas in the potential range of 0 to +1.5V, in presence of scopolamine 50 µM employing 0.1 M phosphate buffer (pH 8). Scan rate: 100 $mV \cdot s^{-1}$.

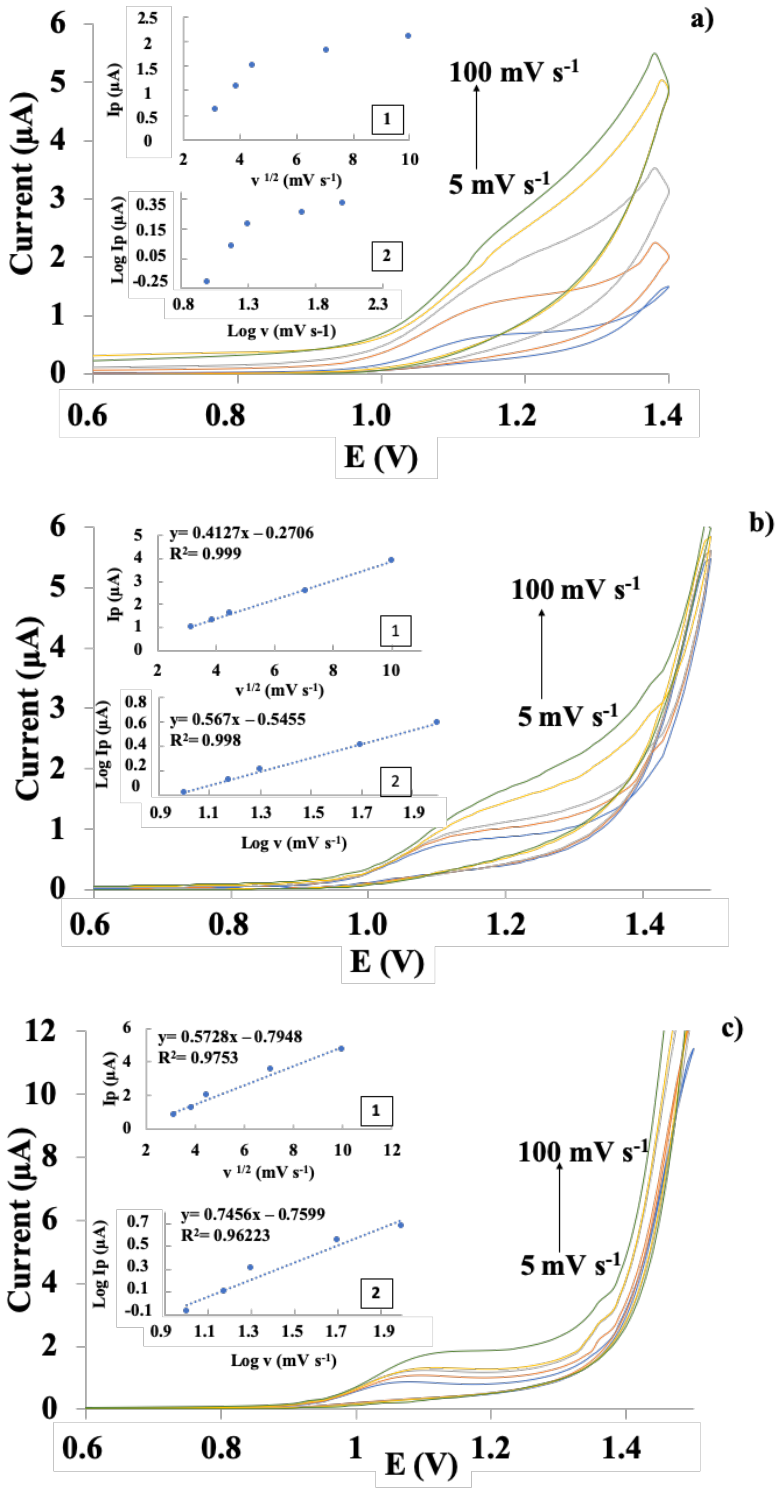

Fig. 6. Cyclic voltammograms of (**a**) SBA-15-MPY, (**b**) HMS-MPY and (**c**) MSU-2-MPY CPEs at different scan rates (from 5 to 100 mV·s^{-1}) performed in 50 µM scopolamine in 0.1 M phosphate buffer (pH 8). Inset **1** shows the relation of the oxidation peak current (I_p) vs. square root of the scan rate ($v^{1/2}$). Inset **2** shows plot of Log Ip vs. Log *v*.

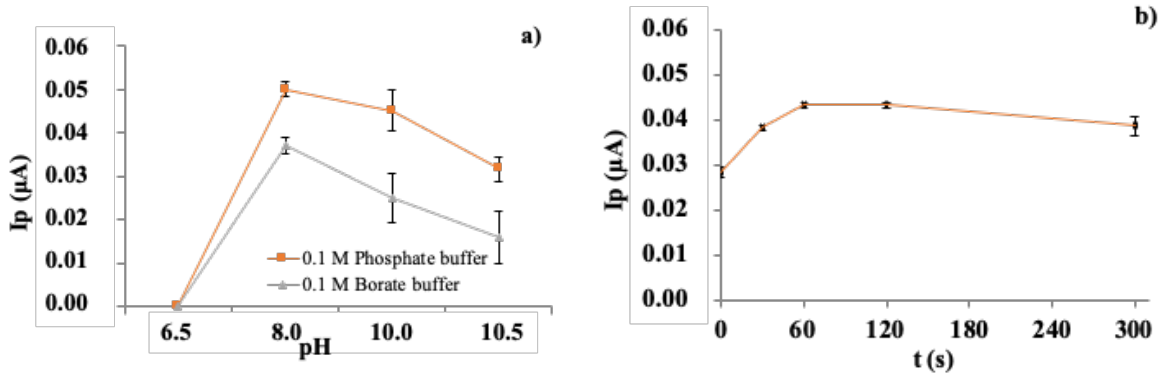

Fig. 7. (a) Effect of electrolyte support and pH value on the peak current of 5 µM scopolamine at HMS-MPY-CPE. (**b)** Effect of accumulation time on the peak current of 5 µM scopolamine at modified CPEs. Scan rate 100 mV s^{-1}.

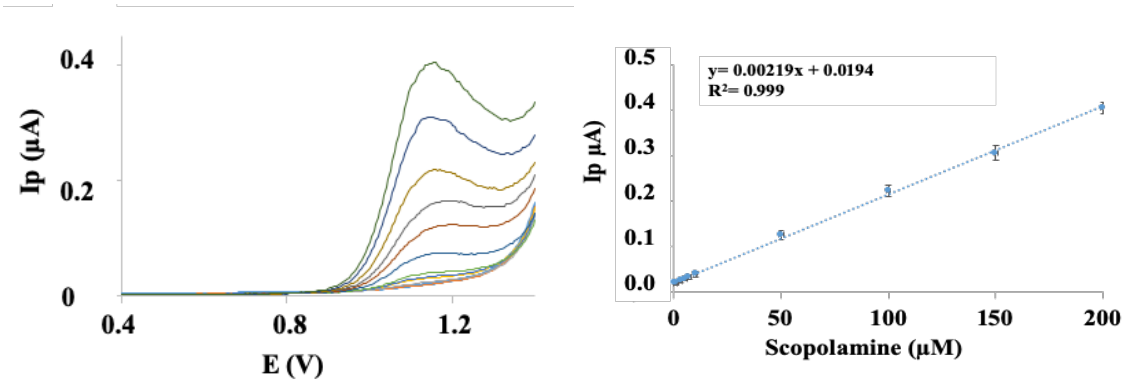

Fig. 8. (a) DPV responses of scopolamine with increasing concentrations in range 0.9 – 200 µM and **(b)** calibration plot of scopolamine. Conditions: 0.1 M phosphate buffer, 1 min accumulation time. Scan rate: 100 $mV \cdot s^{-1}$; pulse amplitude: 10 mV; potential increment: 5 mV; pulse width: 40 ms.

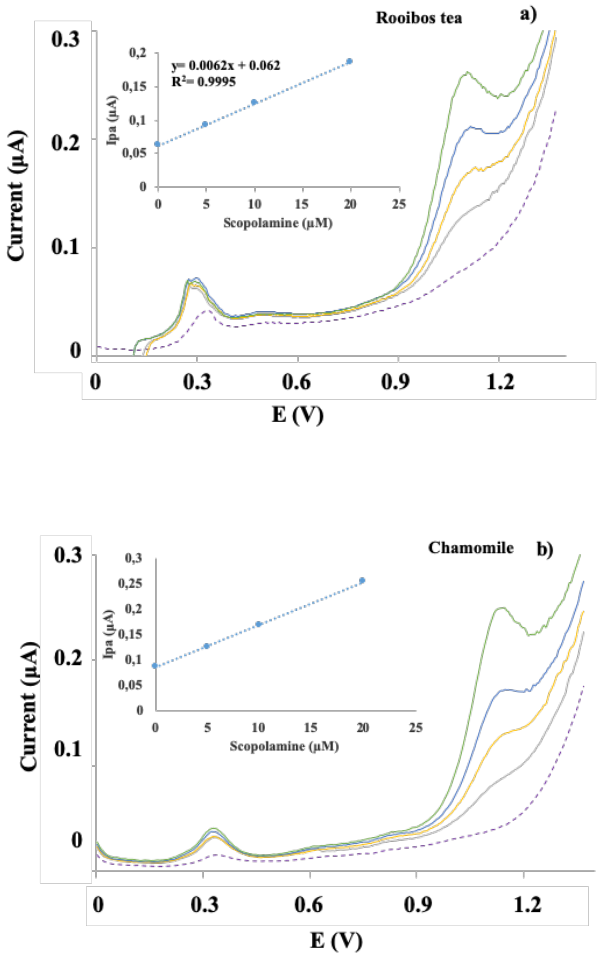

Fig. 9. Differential pulse voltammograms of **(a)** rooibos tea infusion and **(b)** chamomile infusion samples diluted in 0.1 M phosphate buffer (pH 8), before (---) and after (coloured lines) addition of increasing concentrations of scopolamine. Inset in each figure show the respective standard addition calibration plots. Conditions: 0.1 M phosphate buffer, 1 min accumulation time. Scan rate: 100 $mV \cdot s^{-1}$; pulse amplitude: 10 mV; potential increment: 5 mV; pulse width: 40 ms.

Table 1

Characterization data for mesostructured silicas.

Material	2θ (100) (degrees)	Wall thickness (Å)	BET surface area ($m^2\ g^{-1}$)	Pore volume ($cm^3\ g^{-1}$)	BJH pore diameter (Å)	L_0 (mmol g^{-1})	Average particle size (μm)	Particle morphology/ Channel structure
SBA-15	1.06	31.5	780.19	0.80	64.4	-	0.6 x 0.9	Rod-like / 1D hexagonal parallel channels
SBA-15-MPY	1.03	41.9	389.86	0.46	56.8	0.70		Rod-like / 1D hexagonal parallel channels
HMS	2.44	11.0	1078.65	1.02	25.2	-	1.3	Pseudo-spherical/ 3D wormhole like
HMS-MPY	2.42	16.0*	898.44	0.48	**	0.79		Pseudo-spherical/ 3D wormhole like
MSU-2	2.00	13.6	888.48	0.85	33.3	-	1.2	Spherical/3D wormhole like
MSU-2-MPY	1.92	21.0	748.65	0.54	24.9	0.94		Spherical/3D wormhole like

L_0: Millimoles of ligand per gram of material. * Value estimated considering a pore diameter of 20 Å. ** Not calculated

Table 2

Comparison of analytical figure of merits for the determination of scopolamine, in standard solutions, using voltammetric methods.

Technique	Working electrode	Linear range (μM)	Limit of detection (μM)	Reference
SWV	Boron-doped diamond	1-110	0.84	[11]
DPV	Pt electrode	10-1000	0.20	[12]
BIA-SWV	Boron-doped diamond	1 -20	0.12	[13]
DPV	CPE modified with HMS-MPY	1-200	0.30	This work

Table 3

Influence of interference on the voltammetric response of scopolamine on HMS-MPY-CPE.

Interferences	Concentration (μM)	Peak current change (%)
		Scopolamine (10 μM)
Gallic Acid	50	+14.7
Quercetin	50	+13.6
Caffeine	250	0
Atropine	250	0
Na^+	1000	+9.7
K^+	1000	-3.2
Mg^{2+}	1000	+32.3

Table 4 Recoveries obtained for scopolamine determination on HMS-MPY-CPE in tea and herbal tea infusions (n = 3)

Sample	Added (μM)	Total found (μM)	Recovery ± SD (%)
Rooibos tea	0	0	-
	10	9.6	96 ± 3
Green tea	0	0	-
	10	9.2	92 ± 1
Red tea	0	0	-
	10	9.5	95 ± 5
Chamomile	0	0	-
	10	8.5	101 ± 1
Fennel	0	0	-
	10	8.3	83 ± 5